Development 139, 1435-1446 (2012) doi:10.1242/dev.072256

Motor axon exit from the mammalian spinal cord is controlled by the homeodomain protein Nkx2.9 via Robo-Slit signaling

Arlene Bravo-Ambrosio[1], Grant Mastick[2] and Zaven Kaprielian[1,3,*]

SUMMARY

Mammalian motor circuits control voluntary movements by transmitting signals from the central nervous system (CNS) to muscle targets. To form these circuits, motor neurons (MNs) must extend their axons out of the CNS. Although exit from the CNS is an indispensable phase of motor axon pathfinding, the underlying molecular mechanisms remain obscure. Here, we present the first identification of a genetic pathway that regulates motor axon exit from the vertebrate spinal cord, utilizing spinal accessory motor neurons (SACMNs) as a model system. SACMNs are a homogeneous population of spinal MNs with axons that leave the CNS through a discrete lateral exit point (LEP) and can be visualized by the expression of the cell surface protein BEN. We show that the homeodomain transcription factor Nkx2.9 is selectively required for SACMN axon exit and identify the Robo2 guidance receptor as a likely downstream effector of Nkx2.9; loss of Nkx2.9 leads to a reduction in *Robo2* mRNA and protein within SACMNs and SACMN axons fail to exit the spinal cord in *Robo2*-deficient mice. Consistent with short-range interactions between Robo2 and Slit ligands regulating SACMN axon exit, Robo2-expressing SACMN axons normally navigate through LEP-associated Slits as they emerge from the spinal cord, and fail to exit in Slit-deficient mice. Our studies support the view that Nkx2.9 controls SACMN axon exit from the mammalian spinal cord by regulating Robo-Slit signaling.

KEY WORDS: Nkx2.9, Robo, SACMN, Slit, Motor axon exit, Mouse

INTRODUCTION

Motor neurons (MNs) project their axons out of the central nervous system (CNS) and make stereotyped connections with peripheral muscle targets to form circuits that control movement (Bonanomi and Pfaff, 2010; Dalla Torre di Sanguinetto et al., 2008; Sharma and Peng, 2001). Motor axons grow in a directed manner to specialized exit points through which they emerge from the CNS (Bravo-Ambrosio and Kaprielian, 2011; Jacob et al., 2001; Lieberam et al., 2005; Schneider and Granato, 2003; Sharma et al., 1998; Shirasaki and Pfaff, 2002). MN subtypes can be distinguished by the positions of their exit points: ventral MNs (vMNs) and dorsal MNs (dMNs) utilize ventral and dorsal exit points, respectively (Chandrasekhar, 2004; Cordes, 2001; Dillon et al., 2005; Guthrie, 2007; Lieberam et al., 2005; Schubert and Kaprielian, 2001; Sharma et al., 1998; Snider and Palavali, 1990). Although Cxcl12-Cxcr4 signaling regulates the growth of vMN axons to their exit points in mice (Lieberam et al., 2005) and myotomal-derived *diwanka* (*plod3* – ZFIN) glycosyltransferase is required for motor axon growth into the periphery in zebrafish (Schneider and Granato, 2006), the molecular mechanisms that control motor axon exit from the vertebrate spinal cord are poorly understood.

Transcription factors (TFs) control axon pathfinding by regulating the expression of cell surface molecules (Broihier et al., 2004; Garcia-Frigola et al., 2008; Labrador et al., 2005; Landgraf et al., 1999; Lee et al., 2008; Wilson et al., 2008). In *Drosophila*, Zfh1 (Layden et al., 2006) and Nkx6 (HGTX – FlyBase) (Broihier et al., 2004) are required for the exit of vMN axons, whereas Eve (Landgraf et al., 1999) is necessary for dMN axon exit. Nkx6 and Eve are likely to mediate motor axon exit by regulating the expression of Fas3 (Broihier et al., 2004) and Unc5 (Labrador et al., 2005), respectively. In vertebrates, Lhx3/Lhx4 (Sharma et al., 1998) and Phox2b (Hirsch et al., 2007) are required for the directed growth of vMN and dMN axons, respectively, to their exit points. However, these TFs appear to control the specification of vMNs/dMNs rather than motor axon exit per se.

Spinal accessory motor neurons (SACMNs) are branchiomotor dMNs that reside within the cervical spinal cord and project dorsally directed axons to and through a highly localized lateral exit point (LEP) situated midway along the dorsoventral axis of the spinal cord (Dillon et al., 2005; Hirsch et al., 2007; Lieberam et al., 2005). Upon exiting the CNS, SACMN axons execute a rostral turn and assemble into the longitudinally projecting spinal accessory nerve (SAN), which innervates particular neck and back muscles (Dillon et al., 2005; Dillon et al., 2007; Schubert and Kaprielian, 2001; Snider and Palavali, 1990). We identified the immunoglobulin (Ig) domain-containing protein BEN (Alcam or SC1 – Mouse Genome Informatics) (Dillon et al., 2005; Schubert and Kaprielian, 2001) as a selective marker of SACMN cell bodies/axons (Dillon et al., 2005; Schubert and Kaprielian, 2001). Since SACMNs are a molecularly homogenous and readily identifiable population of spinal MNs, which leave the CNS through a circumscribed exit point, they represent an ideal model system for elucidating molecular programs that control motor axon exit.

Our observation that the homeodomain TF Nkx2.9 is likely to be required for SACMN axons to leave the CNS (Dillon et al., 2005) prompted us to further characterize the role of Nkx2.9 in motor axon exit. Here we show that, in mice lacking Nkx2.9, SACMN axons

[1]Dominick P. Purpura Department of Neuroscience, Albert Einstein College of Medicine, Bronx, NY 10461, USA. [2]Department of Biology, University of Nevada, Reno, NV 89557, USA. [3]Department of Pathology, Albert Einstein College of Medicine, Bronx, NY 10461, USA.

*Author for correspondence (zaven.kaprielian@einstein.yu.edu)

Accepted 13 February 2012

appropriately project to the LEP but assemble into an ectopic longitudinally projecting SAN within the spinal cord. We also identify the axon guidance receptor roundabout 2 (Robo2) (Ypsilanti et al., 2010) as a likely downstream effector of Nkx2.9 by showing that Robo2 expression in SACMNs is downregulated in *Nkx2.9* null mice and that SACMN axons fail to exit the spinal cord in *Robo2*-deficient animals. Furthermore, the Robo2 ligands Slit1-3 are present at the LEP, SACMN axons fail to exit the CNS in Slit null mice, and Slit promotes SACMN axon outgrowth in vitro. Collectively, our findings are consistent with Nkx2.9 controlling SACMN axon exit from the CNS by regulating Robo2-Slit interactions at the LEP.

MATERIALS AND METHODS

Mice

CD-1 wild-type (WT) embryos were used for expression studies (Charles River Laboratories). *Nkx2.9* mutant embryos were generated by mating *Nkx2.9*$^{+/-}$ mice and genotypes determined by PCR (Tian et al., 2006). *Nkx2.9* breeding pairs were obtained from J. Locker (Albert Einstein College of Medicine). Pregnant dams were sacrificed as described (Dillon et al., 2005). The morning on which a vaginal plug was detected was considered embryonic day (E) 0.5. Robo and Slit mutant embryos were generated and genotyped as described (Andrews et al., 2008; Farmer et al., 2008; Grieshammer et al., 2004; Long et al., 2004; Lopez-Bendito et al., 2007; Lu et al., 2007; Plump et al., 2002).

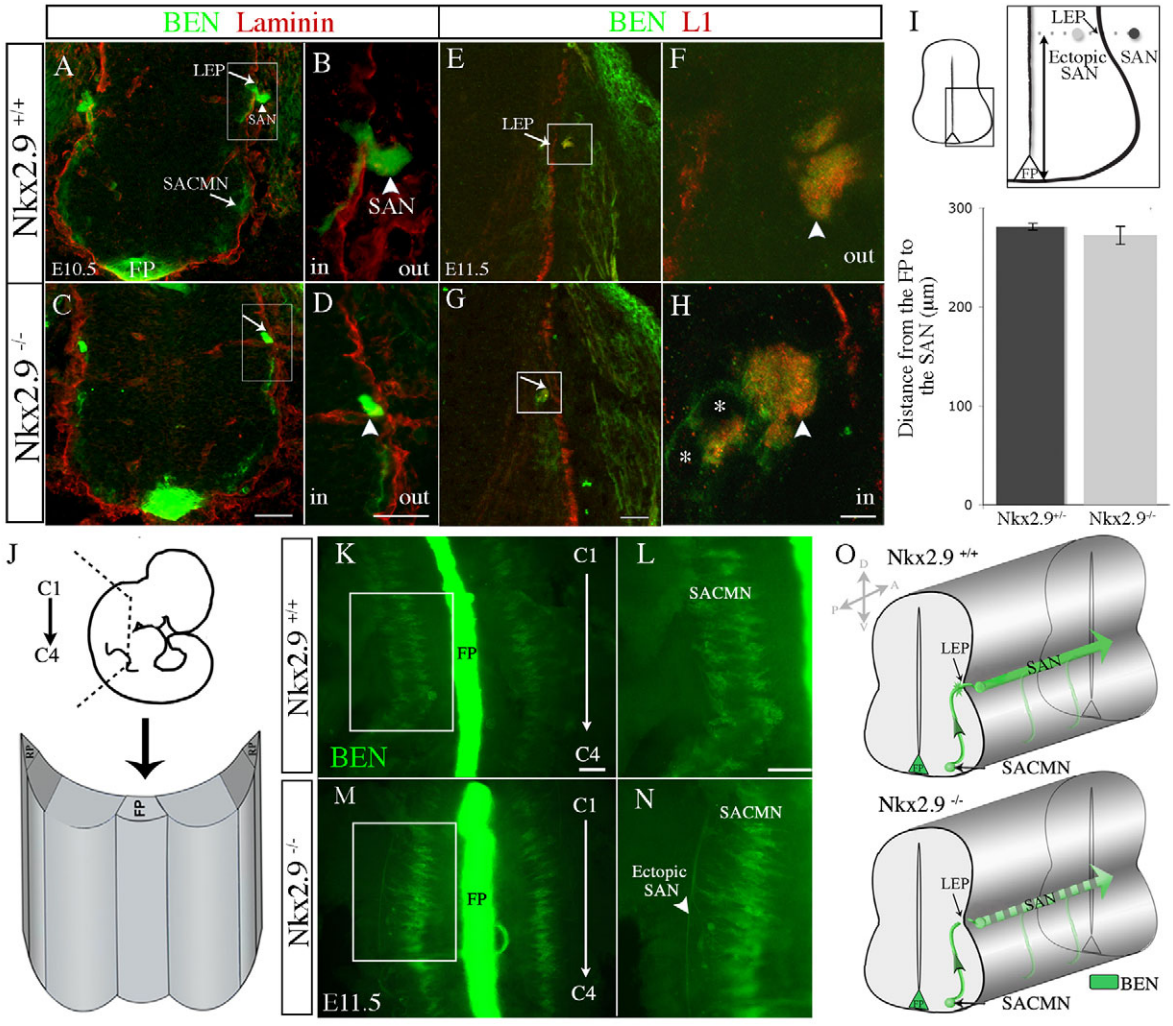

Fig. 1. In *Nkx2.9*$^{-/-}$ embryos, SACMN axons fail to exit the CNS and assemble into an ectopic SAN within the spinal cord. (**A-H**) Wild-type (WT) (A,B, E10.5; E,F, E11.5) and *Nkx2.9*$^{-/-}$ (C,D, E10.5; G,H, E11.5) embryos were labeled with either anti-BEN and anti-laminin (A-D) or anti-BEN and anti-L1 (E-H). (A,B) In E10.5 WT embryos, BEN-labeled spinal accessory motor neuron (SACMN) axons extend through the lateral exit point (LEP) and assemble into a spinal accessory nerve (SAN) located outside the CNS. (C,D) SACMN axons appropriately extend to the LEP in *Nkx2.9*$^{-/-}$ mice but fail to exit and remain within the anti-laminin-labeled margin of the spinal cord (arrow), where they appear to assemble into an ectopic SAN (arrowhead) (n>5). B and D are magnified views of the boxed areas in A and C, respectively. (E-H) A BEN/L1-expressing SAN (arrowhead) forms outside of the spinal cord and adjacent to the LEP (arrow) in WT embryos, whereas in *Nkx2.9*$^{-/-}$ mice the SAN inappropriately forms within the spinal cord adjacent to the LEP and BEN-expressing SACMN (H, asterisks). F and H are magnified views of the boxed areas in E and G, respectively. (**I**) The distance from the base of the floor plate (FP) to the SAN (see upper schematic) was not statistically different in WT (dark gray; SAN) as compared with *Nkx2.9*$^{-/-}$ (light gray; ectopic SAN) embryos (n=4). Error bars indicate s.d. (**J**) Schematized open-book (OB) preparation from cervical levels (C1-C4) of the spinal cord. RP, roof plate. (**K-N**) OB preparations derived from an E11.5 *Nkx2.9* null embryo and a WT littermate labeled with anti-BEN. In contrast to WT embryos (K,L), an ectopic SAN is located within the spinal cord of *Nkx2.9*$^{-/-}$ embryos (M,N; n=3). L and N are magnified views of the boxed areas in K and M, respectively. (**O**) The trajectory of SACMN axons in WT and *Nkx2.9*$^{-/-}$ embryos. Scale bars: 50 μm in C for A,C; 25 μm in D for B,D; 100 μm in G for E,G, in K for K,M, in L for L,N; 5 μm in H for F,H.

RNA isolation, cDNA microarray hybridization, data acquisition and analysis

The Qiagen RNeasy Micro Kit was used to isolate total RNA from E11.5 cervical spinal cords (excluding dorsal spinal cord and floor plate; WT, *n*=3; *Nkx2.9*$^{-/-}$, *n*=3). RNA was amplified using the WT-Ovation Pico RNA Amplification Kit (NuGEN Technologies), followed by hybridization to GeneChip Mouse Genome 430 2.0 Array (Affymetrix) by the Albert Einstein College of Medicine Affymetrix facility. Results from three independent arrays were averaged. The raw data (CEL files) from each probe set were normalized by RMA methods using GeneSpring GX 10.0 software (Agilent). The $\log_2$ transformed signal intensities were averaged for biological replicates and the mean value was used to compute fold change. Differentially expressed genes were identified as those exhibiting a fold change exceeding 1.5, as several previous studies have used this cut-off (Hughes et al., 2000; Schachter et al., 2002; Wang et al., 2003; Yuan et al., 2005) and a fold change of less than 2 can be biologically significant (Hughes et al., 2000).

Immunohistochemistry and in situ hybridization

Antibodies used were: anti-BEN (RIKEN BioResource Center), anti-β-galactosidase (Abcam), anti-NF (DSHB), anti-GFP (Invitrogen), anti-HB9 (S. Pfaff, Salk Institute), anti-Islet1 (DSHB), anti-laminin (Sigma), anti-L1 (Chemicon), anti-myc (Millipore), anti-Phox2b (C. Goridis, INSERM) and anti-Robo2 (R&D Systems). Standard immunohistochemistry, digoxigenin-labeled riboprobe generation and in situ hybridization were carried out as described (Dillon et al., 2005). The mouse *Slit1*, *Slit2*, *Slit3* (Yuan et al., 1999), *Nkx2.9* (Pabst et al., 1998), chick *Robo2* (Reeber et al., 2008) and *BEN* (Dillon et al., 2005) cDNAs were generated as described. Detection of β-galactosidase activity with X-Gal was as described (Corrales et al., 2004). Open-book (OB) spinal cord preparations were generated from E11.5 mouse embryos and subject to whole-mount immunohistochemistry as described (Imondi et al., 2000).

Fluorescent in situ hybridization followed by immunohistochemistry

Cervical spinal cord-containing cryosections derived from E9.5 mouse embryos were hybridized with *Slit1*, *Slit2* or *Slit3* riboprobe for 12 hours at 72°C, and then incubated with anti-digoxigenin POD (Roche) and anti-β-galactosidase (Abcam) overnight at 4°C. Labeled mRNA and protein were visualized using the Tyramide Signal Amplification Plus Cyanine 3 System (Perkin Elmer) and an Alexa Fluor 488-conjugated secondary antibody (Invitrogen), respectively (see Vosshall et al., 2000).

In ovo electroporation

Full-length mouse *Nkx2.9* cDNA was subcloned into the *pMES* expression vector [which contains the chicken β-actin promoter/*CMV-IE* enhancer and *IRES-EGFP* (Swartz et al., 2001)]. Purified *pMES* (2-4 μg/μl), *pMESNkx2.9* (2-4 μg/μl) or cytopcig-Slit1-LRR (0.5 μg/μl) vectors (Shiau

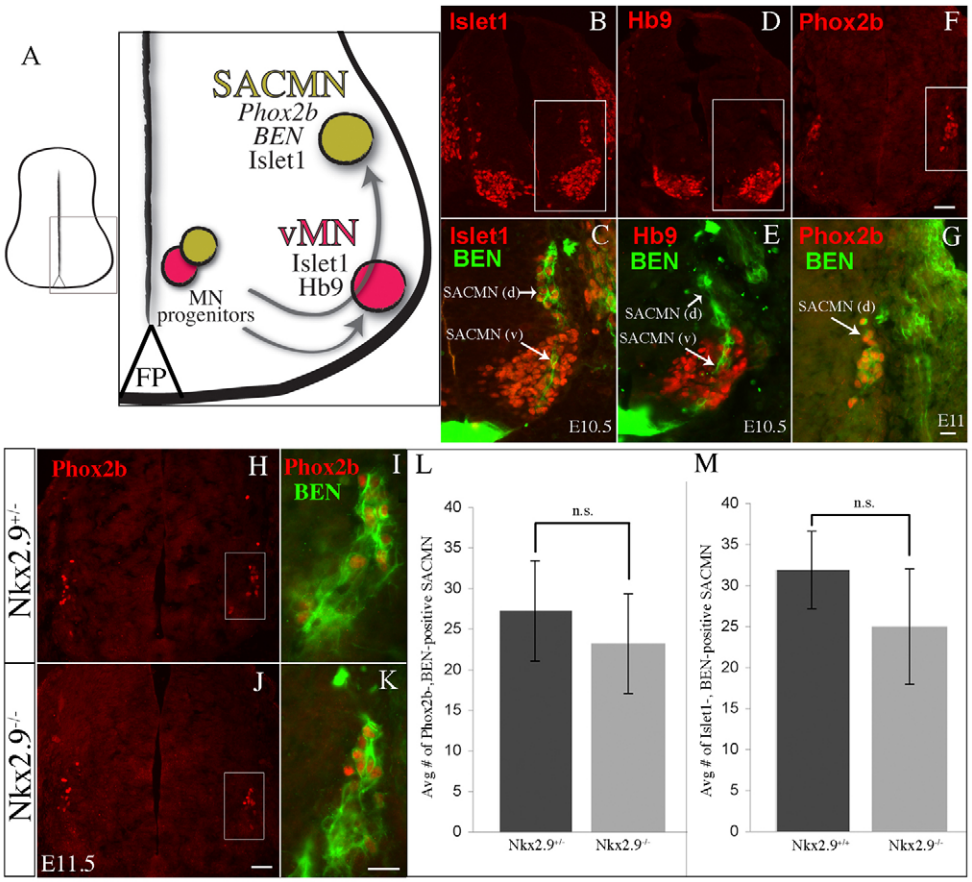

Fig. 2. Appropriate numbers of properly specified SACMNs are formed in *Nkx2.9*-deficient mice. (**A**) Schematic of SACMN and ventral motor neuron (vMN) development in the ventral spinal cord. SACMNs (green circle) and vMNs (red circle) arise from MN progenitors, which migrate away from the ventricular zone to settle in dorsolateral or ventrolateral regions, respectively, of the spinal cord. (**B-G**) Cryosections derived from WT (B-E, E10.5; F,G, E11) embryos labeled with various SACMN or vMN markers show that SACMNs and their axons (arrow) migrate through vMNs [SACMN (v)] and SACMNs that have settled near the LEP [SACMN (d)] and express BEN, Islet1 and Phox2b, whereas vMNs express Islet1 and HB9. C, E and G are magnified views of the boxed areas in B, D and F, respectively. (**H-K**) E11.5 WT (H,I) and *Nkx2.9*$^{-/-}$ (J,K) embryos were labeled with anti-Phox2b (H,J) and colabeled with anti-Phox2b and anti-BEN (I,K). I and K are magnified views of the boxed areas in H and J, respectively. (**L**,**M**) The number of Phox2b$^+$ BEN$^+$ (E11.5; *n*=4) and Islet1$^+$ BEN$^+$ (E10.5; *n*=3) SACMNs is not statistically different between *Nkx2.9*$^{-/-}$ and WT/heterozygote littermates. Error bars indicate s.d. Scale bars: 50 μm in F for B,D,F, in J for H,J; 25 μm in G for C,E,G, in K for I,K.

and Bronner-Fraser, 2009) were microinjected into the central canal of E2 chick embryos, which were then subjected to unilateral electroporation as described (Reeber et al., 2008).

In vitro axon outgrowth assay

Floor plate-containing ventral spinal cord explants were generated from E11.5 WT mouse embryos as described (Imondi and Kaprielian, 2001), placed in 1:1 rat-tail collagen:Matrigel (BD Biosciences) pads and co-cultured with aggregates of mock- or Slit2-transfected (1-2 μg/μl) (Kadison et al., 2006) HEK293 cells for 15-24 hours in 69% OptiMEM with GLUTAMAX (Gibco), 23% F12 (Gibco), 5% FBS (Gemini BioProducts), 2% 2 M glucose and 1% penicillin-streptomycin-glutamine (Gibco). Explants were then fixed in 4% paraformaldehyde for 16 hours at 4°C and subjected to whole-mount immunohistochemistry (Dillon et al., 2005) with anti-BEN (mALCAM antibody, R&D Systems).

Photodocumentation, quantification and statistical analyses

Images were captured and processed as described (Dillon et al., 2005). Confocal images were acquired on a FluoView 500 confocal microscope (Olympus). ImageJ64 software was used to perform measurements. The Mann-Whitney test was performed for all statistical analyses using GraphPad Prism software (version 5.0). Cell body and nerve counts utilized at least five cryosections per animal per genotype. Axon outgrowth was assessed by converting grayscale into binary images using ImageJ64 and outlining areas of equivalent size located between the margins of SACMN axon-containing spinal cord explants and the aggregates of either mock- or Slit2-treated HEK293 cells. The percentage of the delimited area occupied by BEN-positive staining was measured using ImageJ64.

RESULTS

In *Nkx2.9*$^{-/-}$ mice, SACMN axons fail to exit the spinal cord and inappropriately assemble into an ectopic SAN

We previously reported that SACMN axons apparently fail to exit the CNS in *Nkx2.9* null mice (Dillon et al., 2005). To unambiguously determine whether SACMN axons remain confined to the spinal cord in these mice, we labeled transverse cryosections from the cervical spinal cord of E10.5 *Nkx2.9*$^{-/-}$ embryos and their WT littermates with anti-BEN, as a selective marker of SACMNs, and anti-laminin, which demarcates the margin of the spinal cord (Fig. 1A-D). BEN-expressing SACMN axons failed to project across the laminin border in *Nkx2.9*$^{-/-}$ mice (Fig. 1C,D). This does not appear to reflect a developmental delay as SACMN axons do not exit the spinal cord in *Nkx2.9*$^{-/-}$ mice analyzed as late as E13.5, well after SACMN axons normally assemble into the SAN (Dillon et al., 2005) (data not shown).

We next asked whether SACMN axons assemble into an ectopic SAN within the spinal cord of *Nkx2.9* null mice by labeling transverse cryosections from E11.5 embryos with anti-BEN and anti-L1 (L1cam – Mouse Genome Informatics), which labels longitudinally projecting spinal axons (Imondi et al., 2000). A BEN/L1-labeled nerve was located adjacent to the LEP but within the spinal cord in *Nkx2.9*$^{-/-}$ mice (Fig. 1G arrow, 1H arrowhead). To determine whether this ectopic nerve projects along the anterior-posterior (A-P) extent of the cervical spinal cord, we analyzed OB preparations derived from E11.5 *Nkx2.9*$^{-/-}$ and *Nkx2.9*$^{+/+}$ embryos. Consistent with OB preparations lacking an external SAN (Fig. 1J), a BEN-positive SAN was only observed within the spinal cord of *Nkx2.9*$^{-/-}$ mice (Fig. 1K-O). Together, these findings indicate that Nkx2.9 is selectively required for SACMN axon exit. By contrast, vMN axons appropriately emerge from the spinal cord in *Nkx2.9*$^{-/-}$ mice (supplementary material Fig. S1).

Appropriate numbers of SACMNs, which likely arise from Nkx2.9^{+} progenitors, form in *Nkx2.9* null mice

To rule out the possibility that the lack of SACMN axon exit in *Nkx2.9*$^{-/-}$ embryos reflects a reduction in SACMN number, we first identified a panel of SACMN markers by labeling

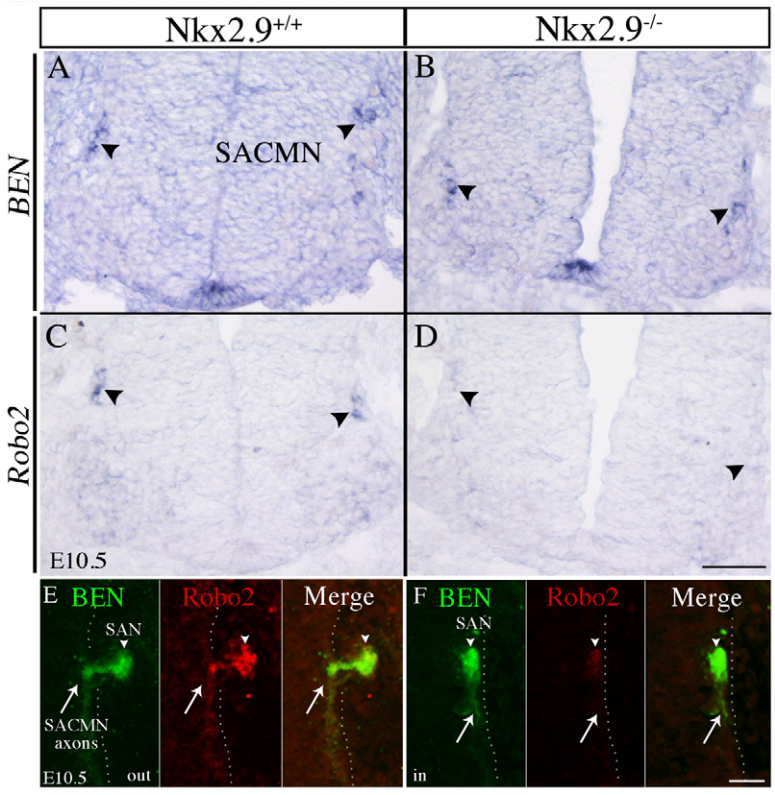

Fig. 3. Robo2 expression is reduced in *Nkx2.9*$^{-/-}$ mice. (**A-F**) E10.5 cryosections derived from WT (A,C,E) or *Nkx2.9*$^{-/-}$ (B,D,F) mice were subjected to in vitro hybridization for *BEN* (*Alcam*) (A,B) or *Robo2* (C,D) mRNA, or labeled with anti-BEN and anti-Robo2 (E,F). Similar levels of *BEN* mRNA are expressed by SACMNs (black arrowheads) in WT (A) and *Nkx2.9*$^{-/-}$ (B) embryos (n>3). SACMN-associated *Robo2* mRNA is reduced in *Nkx2.9*$^{-/-}$ embryos (D; n=3) as compared with WT littermates (C). In *Nkx2.9*$^{-/-}$ embryos, SACMN axons (arrow) and the ectopic SAN (white arrowhead) display reduced levels of Robo2 protein (F; n=3) compared with WT littermates (E). The dotted line indicates the margin of the spinal cord. Scale bars: 100 μm in D for A-D; 25 μm in F for E,F.

cryosections from the cervical spinal cord of WT embryos with anti-BEN and antibodies specific for the MN-associated TFs Islet1 (Ericson et al., 1992; Pfaff et al., 1996), HB9 (Mnx1 – Mouse Genome Informatics) (Arber et al., 1999) or Phox2b (Pattyn et al., 2000). At E10.5-11, BEN-positive SACMNs express the generic MN marker Islet1 (Fig. 2A-C) and the branchiomotor neuron marker Phox2b (Hirsch et al., 2007) (Fig. 2A,F,G), but not HB9 (Fig. 2A,D,E). Therefore, we analyzed the numbers of BEN$^+$ Phox2b$^+$ and BEN$^+$ Islet1$^+$ SACMNs in *Nkx2.9* null and WT littermates and found that appropriate numbers of properly specified SACMNs are generated in the absence of Nkx2.9 (Fig. 2H-M).

To determine whether Nkx2.9 functions cell-autonomously to facilitate SACMN axon exit we compared the distribution of *lacZ*-expressing cells and SACMNs within the spinal cord of a *Nkx2.9-lacZ* knock-in mouse line (Tian et al., 2006). In E9.5 embryos, anti-β-galactosidase staining overlapped with *Nkx2.9* mRNA above the floor plate (FP), suggesting that Nkx2.9$^+$ progenitors give rise to *lacZ*-positive cells (supplementary material Fig. S2A-C). At E10.5, X-Gal staining of sections from *Nkx2.9-lacZ*$^{-/-}$ embryos identified strong labeling above and adjacent to the FP and within cells (presumably SACMNs) that migrate dorsolaterally towards the LEP (supplementary material Fig. S2D). To investigate the possibility that Nkx2.9 is required to maintain the identity of these *lacZ*-positive cells, we labeled cryosections derived from E10.5 *Nkx2.9-lacZ*$^{+/-}$ and *Nkx2.9-lacZ*$^{-/-}$ embryos with anti-β-galactosidase and antibodies to the SACMN markers BEN, Islet1 or Phox2b. β-galactosidase-expressing neurons were labeled by each of these markers (supplementary material Fig. S2E-X), and a subset of β-galactosidase-positive cells within the ventricular zone, which were likely to be Nkx2.9$^+$ progenitors, expressed Phox2b

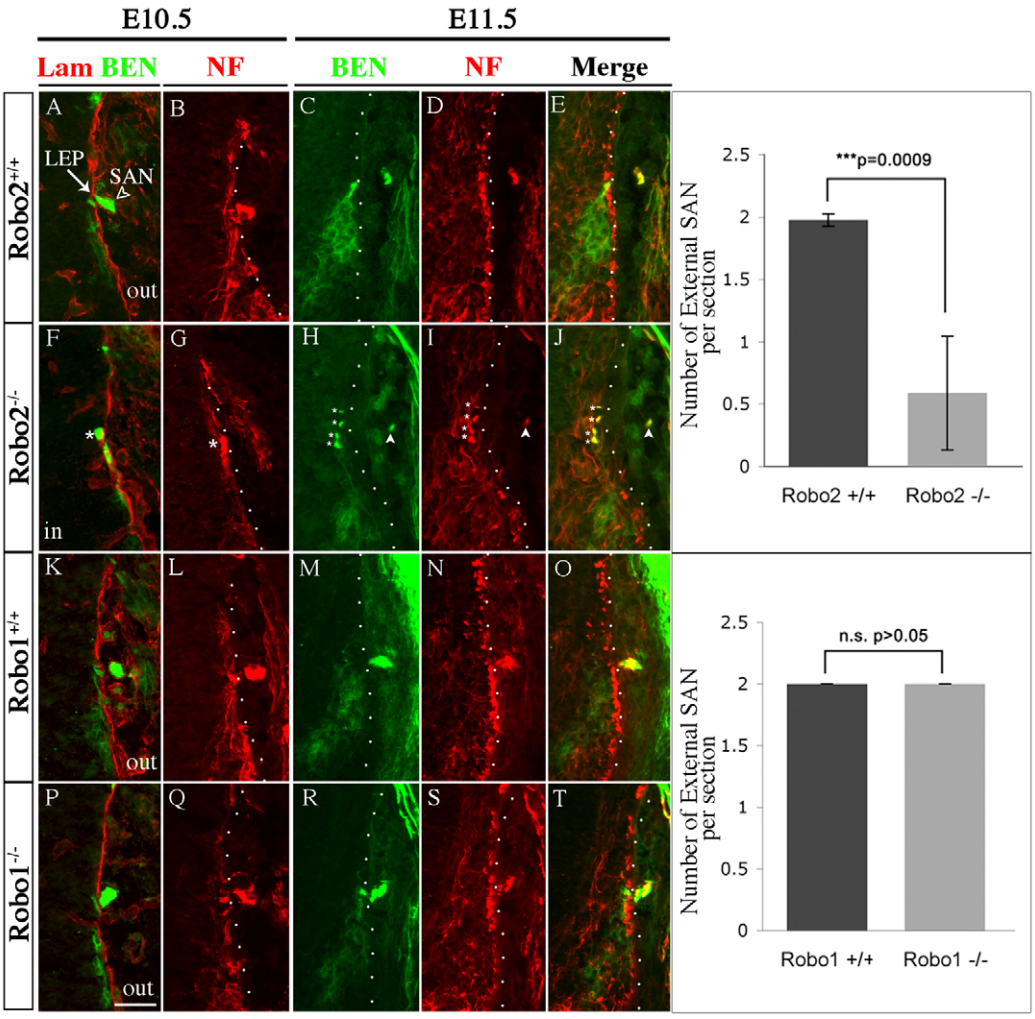

Fig. 4. SACMN axons fail to exit the spinal cord in *Robo2*-deficient mice. (**A-T**) Cryosections derived from E10.5 *Robo2*$^{+/+}$ (A,B), *Robo2*$^{-/-}$ (F,G), *Robo1*$^{+/+}$ (K,L) and *Robo1*$^{-/-}$ (P,Q) embryos were labeled with anti-laminin and anti-BEN (first column) or anti-NF alone (second column). E11.5 *Robo2*$^{+/+}$ (C-E), *Robo2*$^{-/-}$ (H-J), *Robo1*$^{+/+}$ (M-O) and *Robo1*$^{-/-}$ (R-T) embryos were colabeled with anti-BEN (third column) and anti-NF (fourth column). BEN/NF-expressing SACMN axons fail to exit the spinal cord and form an ectopic SAN (asterisk) within the CNS in *Robo2*$^{-/-}$ mice (H-J), whereas in *Robo1*$^{-/-}$ mice (R-T), just as in *Robo2*$^{+/+}$ (C-E) and *Robo1*$^{+/+}$ (M-O) embryos, a SAN (A) formed outside the CNS. As in E10.5 *Robo2*$^{-/-}$ embryos, the majority of BEN/NF-expressing SACMN axons fail to exit the spinal cord at E11.5. At E11.5, several small ectopic SANs (asterisks) form within the spinal cord (H-J), as compared with WT mice (C-E). A small number of SACMN axons emerge from the CNS and form an external SAN at E11.5 (H-J, arrowhead). The bar charts show that the average number of external SANs per section is reduced in E10.5 *Robo2*$^{-/-}$ mice (top; *n*=4), but unaltered in *Robo1*$^{-/-}$ mice (bottom; *n*=3), as compared with WT mice. Error bars indicate s.d. SAN formation is unperturbed in E11.5 *Robo1*$^{-/-}$ mice (R-T; *n*=2), as compared with WT littermates (M-O; *n*=2). Scale bar: 50 μm.

(supplementary material Fig. S2S,U,V,X, asterisk). These observations are consistent with SACMNs arising from a subset of Nkx2.9^{+} progenitors and indicate that the specification/identity of SACMNs is unaltered in *Nkx2.9*$^{-/-}$ mice.

Identifying putative downstream effectors of Nkx2.9

To identify novel downstream effectors of Nkx2.9 that might mediate SACMN axon exit, we used in situ hybridization and immunohistochemistry to examine whether the following known cell surface molecules/axon guidance receptors are expressed by SACMNs: Robo1, Robo2 (Brose et al., 1999; Kidd et al., 1999; Yuan et al., 1999), neuropilin 1 (Npn1) (He and Tessier-Lavigne, 1997; Kolodkin et al., 1997), Npn2 (Chen et al., 1997), NCAM (Ncam1 – Mouse Genome Informatics) (Maness and Schachner, 2007), polysialylated-NCAM (PSA-NCAM) (Boisseau et al., 1991), EphB1-3 (Birgbauer et al., 2001; Holland et al., 1997; Imondi et al., 2000; Jevince et al., 2006; Palmer and Klein, 2003) and VEGFR2 (Kdr – Mouse Genome Informatics) (Ruiz de Almodovar et al., 2009) (data not shown). *Robo2* mRNA expression most closely overlapped with the distribution of SACMNs, and Robo2 protein was present on SACMN axons (see below).

We also carried out an unbiased microarray screen to identify genes dysregulated in *Nkx2.9*$^{-/-}$ embryos (supplementary material Table S1) by comparing total RNA isolated from the ventral half of the cervical spinal cord of E11.5 WT and *Nkx2.9*$^{-/-}$ embryos. This revealed that *Robo2* mRNA levels were ~2-fold lower in *Nkx2.9*-deficient mice than in WT mice (supplementary material Table S1).

Given these findings, we focused our subsequent studies on investigating the regulation of Robo2 expression in *Nkx2.9*$^{-/-}$ embryos and the role of Robo2 in SACMN axon exit.

Robo2 is expressed by SACMNs and is downregulated in *Nkx2.9* null mice

To validate the results of our screens, we labeled cryosections derived from E10.5 *Nkx2.9*$^{-/-}$ embryos and their WT littermates with a *Robo2* riboprobe or anti-Robo2. In WT embryos, BEN-expressing SACMNs express *Robo2* mRNA (Fig. 3A,C, black arrowheads) and Robo2 protein is expressed on SACMN axons (Fig. 3E, arrows) and on the SAN (Fig. 3E, white arrowheads). In *Nkx2.9*$^{-/-}$ embryos, SACMN-associated *Robo2* mRNA levels are reduced (Fig. 3B,D, black arrowheads) and Robo2 protein is downregulated on SACMN axons (Fig. 3F, arrows) that fail to exit the spinal cord, as well as on the ectopic SAN (Fig. 3F, white arrowheads). These observations are consistent with Robo2 operating as a downstream effector of Nkx2.9.

SACMN axons do not exit the spinal cord in *Robo2*-deficient mice

To determine whether Robo2 is required for SACMN axon exit, we labeled E10.5 cryosections derived from *Robo2*$^{-/-}$ mice and their WT littermates with anti-BEN and anti-laminin or anti-neurofilament (NF) (Fig. 4A-J). Phenocopying *Nkx2.9* null mice, the majority of SACMN axons appropriately projected to the LEP but failed to exit the CNS in E10.5 *Robo2*$^{-/-}$ animals (Fig. 4F,G, asterisks), and most SACMN axons remained confined to the spinal cord at E11.5 (Fig. 4H-J). Since a small subset of SACMN axons exited the spinal cord in *Robo2*$^{-/-}$ mice (Fig. 4H-J, arrowheads), we quantified the presence or absence of an external SAN (SACMN axon-containing nerve bundle) on both sides of the spinal cord in WT and *Robo2*$^{-/-}$ embryos. Consistent with the failure of most SACMN axons to exit the CNS, there was a significant reduction in the mean number of external SANs in *Robo2*$^{-/-}$ mice (Fig. 4, top bar chart). Although *Robo1* mRNA is expressed by SACMNs and Robo1 and Robo3 protein is present on the SAN (data not shown), SACMN axon pathfinding/exit is not perturbed in *Robo1* (Fig. 4K-T, bottom bar chart) and *Robo3* (data not shown) null embryos. Accordingly, Robo2 is the sole Robo receptor required for SACMN axon exit from the spinal cord.

Slits are expressed at the LEP and SACMN axon exit is perturbed in Slit null mice

Since SACMN axons appropriately project away from the FP and towards the LEP but fail to exit the spinal cord in *Robo2*$^{-/-}$ mice, short-range interactions between Robo2 and its Slit ligands at the LEP might normally facilitate SACMN axon exit. To test this hypothesis, we labeled serial cryosections derived from E10.5 WT embryos with *Slit1*, *Slit2* or *Slit3* riboprobes (Fig. 5A-D). High levels of *Slit2* and lower levels of *Slit1* and *Slit3* are present at the LEP, and each Slit gene is expressed in vMNs and the FP. Based on these observations, we analyzed SACMN axon pathfinding in mice lacking one or more Slits by labeling cryosections from E10.5 *Slit1*$^{-/-}$, *Slit2*$^{-/-}$ or *Slit1*$^{-/-}$ *Slit2*$^{-/-}$ embryos with anti-BEN and anti-NF. Whereas SACMN axon pathfinding/exit was not perturbed in the absence of Slit1 (Fig. 6D-F′) or Slit2 (Fig. 6G-I′), SACMN axons failed to exit the spinal cord in mice lacking both Slit1 and Slit2 (Fig. 6J-L′). In the double-mutant mice, SACMN axons formed more than one ectopic SAN within the spinal cord, just as they do in *Robo2*$^{-/-}$ mice (Fig. 6J-L′, asterisks). The number of ectopic nerve bundles was significantly increased, and there was a corresponding reduction in the number of normally positioned external SANs, in *Slit1*$^{-/-}$ *Slit2*$^{-/-}$ embryos as compared with WT mice and mutant mice lacking other combinations of Slits (Fig. 6M,N). These findings identify Slit1 and Slit2 as the LEP-associated Robo2 ligands required

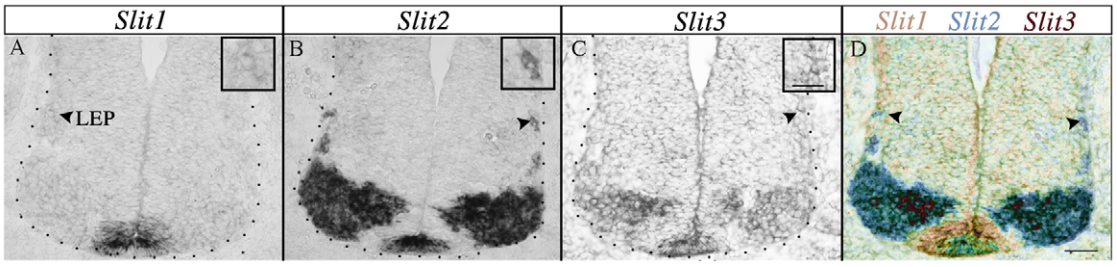

Fig. 5. Distribution of Slit mRNA in the cervical spinal cord. (**A-D**) Serial cryosections derived from E10.5 WT embryos were labeled with *Slit1* (A), *Slit2* (B) or *Slit3* (C) riboprobes. (D) Pseudo-color image representing the merge of A-C. High levels of *Slit2* (B,D, arrowheads) and low levels of *Slit1* and *Slit3* are expressed at the LEP (A,C,D). High-magnification micrographs depicting LEP-associated expression are included as insets (A-C, arrowheads). Dotted lines demarcate spinal cord margin. Scale bar: 50 μm.

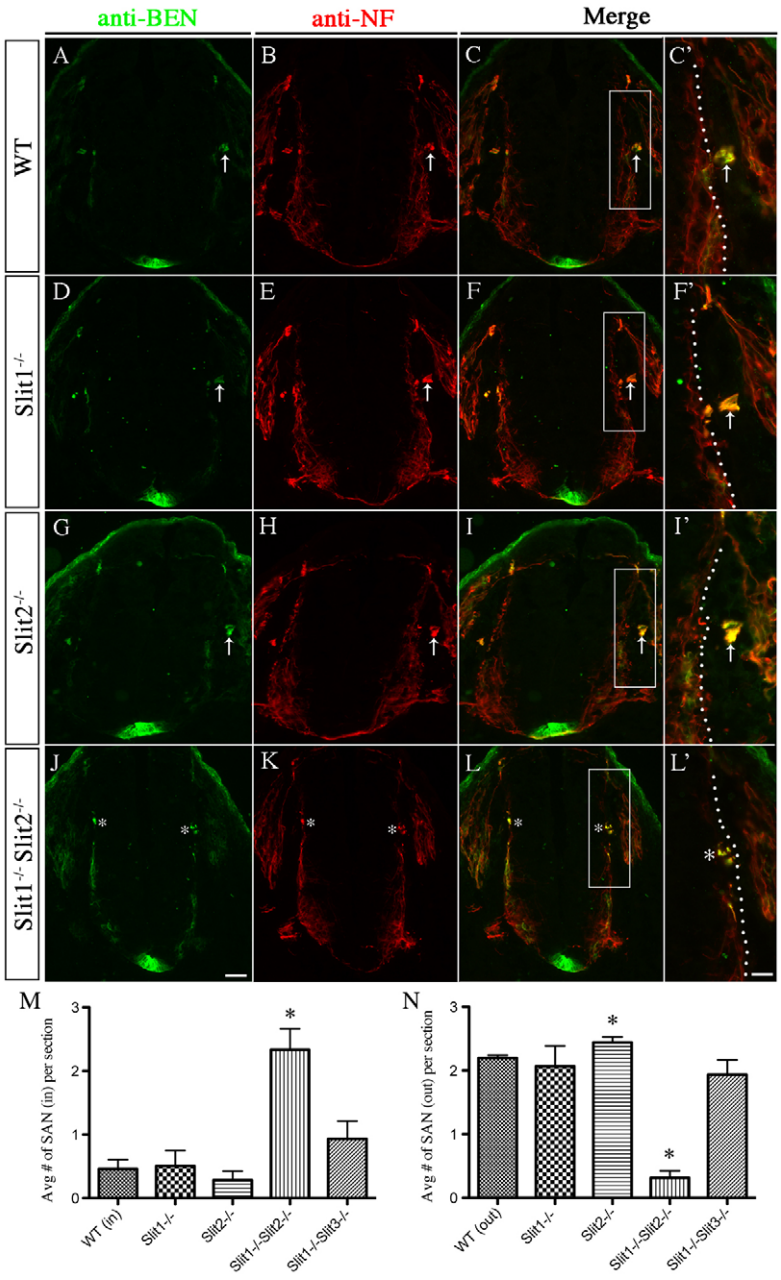

Fig. 6. SACMN axon exit is perturbed in *Slit1*$^{-/-}$ *Slit2*$^{-/-}$ mice. (**A-L′**) Cryosections derived from E10.5 WT (A-C′) and Slit mutant (D-L′) embryos were labeled with anti-NF and anti-BEN. SACMN axons appropriately exit the spinal cord and assemble into an external SAN (arrow) in WT (A-C′; E10.5, *n*>5; E11.5, *n*>5), *Slit1*$^{-/-}$ (D-F′; E10.5, *n*=5; E11.5, *n*=9; data not shown), *Slit2*$^{-/-}$ (G-I′; E10.5, *n*=1; E11.5, *n*=3) or *Slit1*$^{-/-}$ *Slit3*$^{-/-}$ (E11.5, *n*=3; data not shown) mice. (**M**,**N**) The average number of SANs located inside or outside of the spinal cord is not statistically different between *Slit1*$^{-/-}$ mutant, *Slit1*$^{-/-}$ *Slit3*$^{-/-}$ mutant and WT mice. Notably, in *Slit1*$^{-/-}$ *Slit2*$^{-/-}$ mice, SACMN axons fail to exit the CNS and instead assemble into an ectopic SAN (J-L′, asterisks). The average number of SANs outside the spinal cord in *Slit2*$^{-/-}$ mice is significantly increased compared with WT embryos (N). **P*<0.05; error bars indicate s.e.m. E10.5, *n*=3; E11.5, *n*=3; E11.5 data not shown. Scale bars: 50 μm in J for A-C,D-F,G-I,J-L; 25 μm in L′ for C′,F′,I′,L′.

for SACMN axon exit, and suggest that the increase in the number of ectopic nerves within *Slit1*$^{-/-}$ *Slit2*$^{-/-}$ mice might arise from defasciculation of longitudinally projecting SACMN axons.

Our expression and genetic data raise the possibility that short-range interactions between Robo2-expressing SACMN axons and LEP-associated Slits normally facilitate SACMN axon exit. Since SACMN cell bodies eventually settle near the LEP (Dillon et al., 2005), it is possible that they themselves might represent the source of Slit mRNA expression. We tested this hypothesis by colabeling cryosections derived from E9.5 *Nkx2.9-lacZ*$^{+/-}$ embryos with *Slit1*, *Slit2* or *Slit3* riboprobes and anti-β-galactosidase to visualize Nkx2.9^{+} progenitor-derived SACMNs (supplementary material Fig. S2). At E9.5, when the majority of SACMN axons have reached the LEP but have yet to exit the spinal cord, LEP-associated *Nkx2.9-lacZ*-expressing SACMNs do not express Slit mRNA (Fig. 7A-I, arrowheads). By contrast, SACMNs are likely to express Slit as they begin to migrate away from the FP (Fig. 7A-I). Together, our data suggest that short-range interactions between Slits expressed by LEP-associated (non-SACMN) cells and Robo2-expressing SACMN axons facilitate SACMN axon exit. To determine whether SACMN axons are attracted or repelled by Slits in vitro, we co-cultured SACMN-containing embryonic mouse spinal cord explants and aggregates of Slit2-expressing HEK293 cells. Anti-BEN-labeled SACMN axons exhibited more robust outgrowth towards Slit2-expressing HEK293 cells than towards mock-transfected HEK293 cells (Fig. 8). Therefore, short-range attractive Robo2-Slit interactions at the LEP are likely to promote SACMN axon exit (Fig. 10).

Given that multiple ectopic SANs appear to form in *Robo2*$^{-/-}$ and *Slit1*$^{-/-}$ *Slit2*$^{-/-}$ mice, we asked whether these nerves appropriately project along the A-P axis of the spinal cord by labeling OB preparations derived from the cervical spinal cord

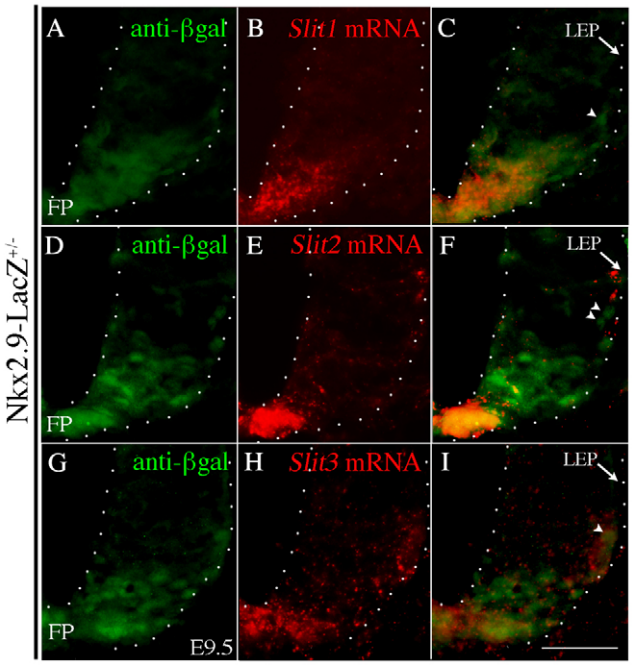

Fig. 7. LEP-associated cells express Slits. (**A-I**) Serial cryosections derived from E9.5 *Nkx2.9-lacZ*$^{+/-}$ mouse embryos were colabeled with anti-β-galactosidase and *Slit1* (A-C), *Slit2* (D-F) or *Slit3* (G-I) riboprobe. LEP-associated (arrow) cells, but not *Nkx2.9-lacZ*-expressing SACMNs (arrowheads), express Slits. Scale bar: 50 μm.

of these mice with anti-BEN (Fig. 9A-D). These analyses revealed that SACMN axons form disorganized nerve fascicles along the A-P axis of the spinal cord in mice lacking either Robo2 or Slit1/2 (Fig. 9C,D, arrows), supporting a role for Robo2-Slit interactions in the proper growth of longitudinally projecting SACMN axons.

DISCUSSION

The projection of motor axons out of the CNS is a key, but poorly understood, phase of MN development (Bonanomi and Pfaff, 2010; Hirsch et al., 2007; Lieberam et al., 2005; Schneider and Granato, 2003; Shirasaki and Pfaff, 2002; Vermeren et al., 2003). Here we describe the first identification of a genetic program that regulates spinal motor axon exit in vertebrates.

Nkx2.9 controls SACMN axon exit

We show that SACMN axons appropriately project to the LEP but fail to exit the spinal cord in *Nkx2.9*$^{-/-}$ mice. This indicates that Nkx2.9 is not required for the pathfinding of SACMN axons within the spinal cord and suggests that the FP-derived chemorepellent netrin 1 directs Unc5-expressing SACMN axons away from the FP (Dillon et al., 2005; Dillon et al., 2007) and that LEP-associated chemoattractants (Caton et al., 2000; Guthrie and Lumsden, 1992), possibly secreted by boundary cap cells at motor exit points (Bron et al., 2007; Maro et al., 2004; Mauti et al., 2007; Vermeren et al., 2003), are likely to guide SACMN axons to the LEP. Since normal numbers of properly specified SACMNs are present in *Nkx2.9*$^{-/-}$ mice (Fig. 2 and supplementary material Fig. S2), and *Nkx2.9*$^{-/-}$ mice display WT-like ventral spinal cord patterning (Pabst et al., 2003), Nkx2.2 is likely to operate redundantly with Nkx2.9 to control the specification/differentiation of SACMNs (Dillon et al., 2005; Pabst et al., 2003). Although Nkx2.9^{+} progenitors are capable of differentiating into interneurons (Briscoe et al., 1999; Holz et al., 2010; Pabst et al., 2003), our data indicate that a subset express SACMN markers, suggesting that Nkx2.9 regulates SACMN axon exit in a cell-autonomous manner. Given that *Nkx6* is required for vMN axon exit from the *Drosophila* ventral nerve cord (Broihier et al., 2004), Nkx TFs might have evolutionarily conserved roles in motor axon exit.

Nkx2.9 regulates Robo2 expression

Nkx genes encode homeodomain-containing TFs that regulate cell type specification and organogenesis (Briscoe et al., 2000; Briscoe et al., 1999; Harvey, 1996; Stanfel et al., 2005), and Nkx2.9 is required for FP development and commissural axon guidance (Holz et al., 2010). We show that SACMN-associated *Robo2* mRNA and protein are reduced in *Nkx2.9*$^{-/-}$ embryos, identifying Robo2 as the first candidate CNS-associated downstream effector of any vertebrate Nkx gene. By contrast, we observed no changes in Slit mRNA expression in these animals (data not shown). Although the presence of putative Nkx2 binding sites within the *Robo2* promoter (data not shown) is consistent with *Robo2* being a direct target of Nkx2.9, forced expression of Nkx2.9 does not modulate Robo2 expression (supplementary material Fig. S3).

Robo2 and Slit1/2 are required for SACMN axon exit

Our findings are the first to show that Robo2-Slit signaling is required to facilitate motor axon exit from the spinal cord. Since Slit2 appears to be the most abundant LEP-associated Slit, it was

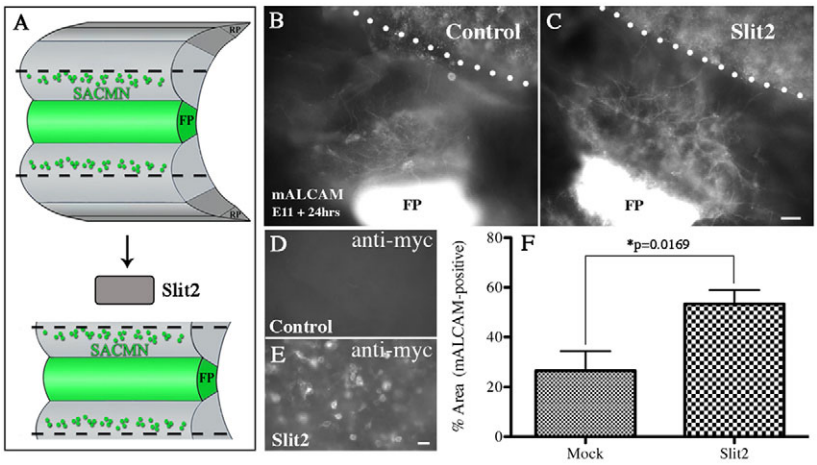

Fig. 8. Slits promote SACMN axon outgrowth in vitro. (**A**) Schematic depicting the generation of SACMN-containing spinal cord explants and their co-culture with aggregates of Slit2-expressing HEK293 cells. (**B**,**C**) Explants were co-cultured with either mock-transfected (B; *n*=17; limited axon outgrowth) or Slit2-expressing (C; *n*=10/13 explants showed significant axon outgrowth) HEK293 cells and labeled with anti-BEN (anti-mALCAM; note that this antibody non-specifically labels HEK293 cells). (**D**,**E**) Anti-myc labels aggregates of Slit2-expressing (E) but not mock-transfected (D) HEK293 cells. (**F**) The percentage of the area between SACMN-containing explants and HEK293 aggregates that is anti-BEN-positive is significantly greater for Slit2-expressing than for mock-transfected cells. Error bars indicate s.e.m.; $n \geq 5$. Scale bars: 50 μm in C for B,C; 25 μm in E for D,E.

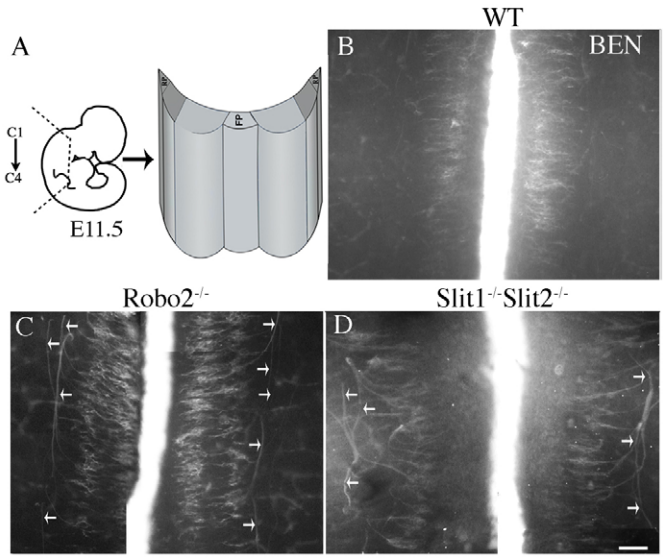

Fig. 9. SAN formation is perturbed in *Robo2*$^{-/-}$ and *Slit*$^{-/-}$ *Slit2*$^{-/-}$ mice. (**A**) Schematic of an OB preparation isolated from the cervical spinal cord. (**B-D**) E11.5 OB preparations derived from WT (B), *Robo2*$^{-/-}$ (C) and *Slit1*$^{-/-}$ *Slit2*$^{-/-}$ (D) embryos were labeled with anti-BEN. Unlike WT mice (B; *n*>4), BEN-expressing axons assembled into disorganized nerve fascicles (arrows), within the spinal cord, in *Robo2*$^{-/-}$ (C; *n*=6) and *Slit1*$^{-/-}$ *Slit2*$^{-/-}$ (D; *n*=3) mice. Scale bar: 50 μm.

surprising to find that SACMN axons appropriately exit the spinal cord in mice lacking Slit2. Possible explanations for these observations are that low levels of Slit1 are capable of facilitating SACMN axon exit and/or that Slit1 and Slit2 operate redundantly to regulate exit. The finding that SACMN axons do not exit the spinal cord in *Slit1*$^{-/-}$ *Slit2*$^{-/-}$ mice further indicates that LEP-associated Slit3 does not promote SACMN axon exit on its own. Nevertheless, in the absence of published data indicating that Robo2 binds each of the vertebrate Slits with different affinities, it is difficult to reconcile why Slit1, but not Slit3, appears to compensate for the loss of Slit2. In contrast to our loss-of-function data, misexpression of Slits in the chick spinal cord does not perturb SACMN axon pathfinding (supplementary material Fig. S4).

Robo-Slit signaling regulates the guidance of longitudinally projecting axons in the developing mouse brain stem (Dugan et al., 2011; Farmer et al., 2008; Mastick et al., 2010), forebrain (Devine and Key, 2008; Ricano-Cornejo et al., 2011) and spinal cord (Reeber et al., 2008). Consistent with these observations, we show that Robo2 and both Slit1 and Slit2 are required for the proper assembly of SACMN axons into the SAN. Whereas SACMN axons form an organized ectopic nerve bundle in *Nkx2.9*$^{-/-}$ embryos, disorganized/tangled nerve fascicles are present within the spinal cord of *Robo2*$^{-/-}$ and *Slit1*$^{-/-}$ *Slit2*$^{-/-}$ mice. Ventral spinal cord (including vMN)-associated Slits (Brose et al., 1999; Kadison et al., 2006; Yuan et al., 1999) might play a key role in constraining the orientation of longitudinally projecting SACMN axons as Slit1 and Slit2 position retinal ganglion cell axons at the optic chiasm (Plump et al., 2002).

The dynamic role of Robo-Slit interactions in SACMN axon pathfinding

Given that the Slit-rich FP and ventral spinal cord would be expected to represent repulsive territories for Robo2-expressing SACMN axons, how are these axons capable of growing away from the FP and through the ventral spinal cord (Fig. 10A)? As is the case for vMNs (Bai et al., 2011; Brose et al., 1999), SACMNs are likely to co-express Robo2 and Slits as their axons navigate these initial segments of their trajectory (Figs 7, 10). Thus, Slits produced by SACMN cell bodies might occupy SACMN axon-associated Robo receptors, rendering them insensitive to FP- and ventral spinal cord-associated Slits, analogous to the co-expression of Slit and Robo in vMNs inhibiting the responsiveness of their

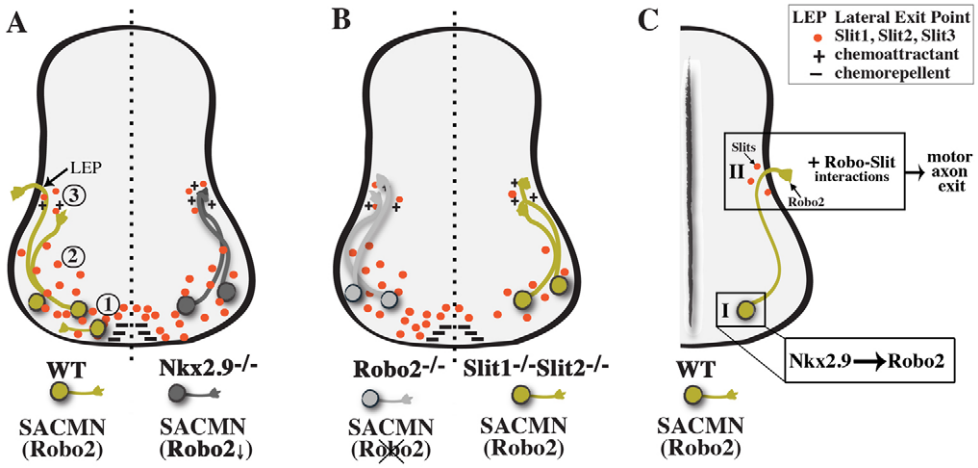

Fig. 10. A model for the dynamic role of Robo2-Slit interactions in regulating SACMN axon pathfinding towards and through the LEP. (**A**,**B**) In WT mice (A, left), Robo2-expressing (Robo2) SACMN axons (green) navigate in close proximity to three sources of Slits (red circles) as they extend away from the FP (1), grow through vMNs (2), and project to and through the LEP (3). SACMNs express Robo2 and Slits as they pathfind away from the FP and traverse vMNs, and through potential cis attenuation of Robo2-Slit signaling their axons become insensitive to FP- and vMN-derived Slits (1, 2). SACMN axons are normally repelled by the FP-derived chemorepellent Netrin (–) and could be guided to the LEP by exit point-derived chemoattractants (+). Once Robo2-positive SACMN axons reach the LEP, they no longer express Slits, become responsive to LEP-associated Slits (3), and attractive Robo2-Slit interactions facilitate their exit from the spinal cord. By contrast, SACMN axons in *Nkx2.9*$^{-/-}$ (dark gray, Robo2↓, A right), *Robo2*$^{-/-}$ (light gray, Robo2, B left) and *Slit1*$^{-/-}$ *Slit2*$^{-/-}$ (green, Robo2, B right) mice appropriately reach the LEP but fail to exit the spinal cord. (**C**) Model for Nkx2.9 control of SACMN axon exit via Robo-Slit signaling. (I) Nkx2.9 regulates Robo2 expression in SACMNs. (II) Attractive short-range Robo2-Slit interactions at the LEP facilitate SACMN axon exit from the CNS.

axons to Netrin (Bai et al., 2011). Similarly, co-expression of Sema3A and Npn1 on vMNs prevents their axons from responding to exogenous Sema3A (Moret et al., 2007), and the attenuation of Eph receptor signaling via ephrins in cis alters the responsiveness of vMN axons to trans ephrins (Kao and Kania, 2011).

Our observations suggest that short-range, presumably attractive/positive (Fig. 8) interactions between Robo2-expressing SACMN axons and LEP-associated Slits promote SACMN axon exit from the spinal cord. Consistent with this possibility, mesodermal cells (Kramer et al., 2001) and tracheal branches (Englund et al., 2002) are attracted to Slit in *Drosophila* embryos, and human leukocytes are attracted to a Slit source in vitro (Ye et al., 2010). *Drosophila* mesodermal cells are also capable of responding to Slit as both an attractant and repellent during sequential phases of their migration (Kramer et al., 2001). By analogy, SACMN axons might alter their responsiveness to LEP-associated Slits, first perceiving Slits as attractants and then as repellents, and this would ultimately push SACMN axons out of the spinal cord. We favor the possibility that Slits produced by LEP-associated cells facilitate SACMN axon exit; however, Robo2-expressing SACMN axons could transport ventral midline-associated Slits to the LEP, just as the Frazzled receptor captures and redistributes its Netrin ligand to modulate axon pathfinding within the *Drosophila* CNS (Hiramoto et al., 2000). Selectively eliminating Slits from LEP-associated cells would clarify which sources of Slits are required for SACMN axon exit.

To ultimately emerge from the spinal cord, motor axons must break through the basement membrane surrounding the neural tube. Although our studies do not directly address this aspect of SACMN axon pathfinding, it seems plausible that Robo2-Slit interactions promote cytoskeletal remodeling, which might alter the shape of SACMN growth cones and facilitate exit. Consistent with this possibility, the complexity of SACMN axon-associated growth cones is dramatically reduced as they exit the LEP (Snider and Palavali, 1990), and this might facilitate their passage through small ‘gaps’ formed by glial end-feet at motor exit points (Fraher et al., 2007).

Alternatively, Slit activation of Robo2 at the LEP might trigger the release of either soluble or membrane-bound proteolytic enzymes such as matrix metalloproteinases (MMPs) (McFarlane, 2003), which are capable of breaking down the basal lamina and potentially promoting SACMN axon exit. Our microarray results indicate that the expression of the ADAM metallopeptidase *Adamts3* is reduced in *Nkx2.9*$^{-/-}$ mice, raising the possibility that MMPs might regulate SACMN axon exit (supplementary material Table S1). In one scenario, SACMN axons may extend small, localized protrusions termed invadopodia that selectively secrete MMPs, which degrade the basement membrane (Bravo-Ambrosio and Kaprielian, 2011). No matter how SACMN axons break through the border between the CNS and the peripheral nervous system, we have provided evidence that short-range Robo2-Slit interactions are likely to regulate this crucial phase of motor axon development.

Acknowledgements

We thank Deyou Zheng and Xingyi Guo (Albert Einstein College of Medicine) for assistance with analyses of microarray data; William Andrews (University of London) and Marc Tessier-Lavigne (Genentech) for mutant mice; Minkyung Kim and Brielle Bjorke (University of Nevada) for genotyping; and the following investigators for plasmids: Cathy Krull (University of Michigan; *pMES*), Hans-Henning Arnold (University of Braunschweig, Germany; mouse *Nkx2.9*), Marianne Bronner-Fraser (California Institute of Technology; cytopcig-Slit1-LRR), Yi Rao (National Institute of Biological Sciences; Slit2) and Marc Tessier-Lavigne (Robo3 probe). We also thank William Andrews, Jean Hebert, Hannes Buelow, Joseph Locker, Roy Sillitoe and Nozomi Sakai (Albert Einstein College of Medicine) for critical comments on the manuscript. Monoclonal antibodies specific for NF (T. M. Jessell and J. Dodd) and Islet1 (T. M. Jessell and S. Brenner-Morton) were obtained from the Developmental Studies Hybridoma Bank developed under the auspices of the NICHD and maintained by The University of Iowa, Department of Biology, Iowa City, IA 52242, USA.

Funding

This work was supported by National Institutes of Health (NIH) grants [R56NS038505 and R01NS038505 to Z.K., RO1 NS054740, RR024210 and GM103554 to G.M.]. A.B.-A. was supported by fellowships from the Einstein Medical Scientist Training Program and Society for Neuroscience’s Neuroscience Scholars Program, and an Edward A. and Lucille Kimmel Scholarship. Deposited in PMC for release after 12 months.

Competing interests statement

The authors declare no competing financial interests.

Supplementary material

Supplementary material available online at
http://dev.biologists.org/lookup/suppl/doi:10.1242/dev.072256/-/DC1

References

Andrews, W., Barber, M., Hernadez-Miranda, L. R., Xian, J., Rakic, S., Sundaresan, V., Rabbitts, T. H., Pannell, R., Rabbitts, P., Thompson, H. et al. (2008). The role of Slit-Robo signaling in the generation, migration and morphological differentiation of cortical interneurons. *Dev. Biol.* **313**, 648-658.

Arber, S., Han, B., Mendelsohn, M., Smith, M., Jessell, T. and Sockanathan, S. (1999). Requirement for the homeobox gene Hb9 in the consolidation of motor neuron identity. *Neuron* **23**, 659-674.

Bai, G., Chivatakarn, O., Bonanomi, D., Lettieri, K., Franco, L., Xia, C., Stein, E., Ma, L., Lewcock, J. W. and Pfaff, S. L. (2011). Presenilin-dependent receptor processing is required for axon guidance. *Cell* **144**, 106-118.

Birgbauer, E., Oster, S. F., Severin, C. G. and Sretavan, D. W. (2001). Retinal axon growth cones respond to EphB extracellular domains as inhibitory axon guidance cues. *Development* **128**, 3041-3048.

Boisseau, S., Nedelec, J., Poirier, V., Rougon, G. and Simonneau, M. (1991). Analysis of high PSA-NCAM expression during mammalian spinal cord and peripheral nervous system development. *Development* **112**, 69-82.

Bonanomi, D. and Pfaff, S. L. (2010). Motor axon pathfinding. *Cold Spring Harb. Perspect. Biol.* **2**, a001735.

Bravo-Ambrosio, A. and Kaprielian, Z. (2011). Crossing the border: molecular control of motor axon exit. *Int. J. Mol. Sci.* **12**, 8539-8561.

Briscoe, J., Sussel, L., Serup, P., Hartigan-O’Connor, D., Jessell, T. M., Rubinstein, J. L. and Ericson, J. (1999). Homeobox gene Nkx2.2 and specification of neuronal identity by graded Sonic hedgehog signalling. *Nature* **398**, 622-627.

Briscoe, J., Pierani, A., Jessell, T. M. and Ericson, J. (2000). A homeodomain protein code specifies progenitor cell identity and neuronal fate in the ventral neural tube. *Cell* **101**, 435-445.

Broihier, H. T., Kuzin, A., Zhu, Y., Odenwald, W. and Skeath, J. B. (2004). *Drosophila* homeodomain protein Nkx6 coordinates motoneuron subtype identity and axonogenesis. *Development* **131**, 5233-5242.

Bron, R., Vermeren, M., Kokot, N., Little, G. E., Mitchell, K. J., Andrews, W. and Cohen, J. (2007). Boundary cap cells constrain spinal motor neuron somal migration at motor exit points by a semaphorin-plexin mechanism. *Neural Dev.* **2**, 21.

Brose, K., Bland, K. S., Wang, K. H., Arnott, D., Henzel, W., Goodman, C. S., Tessier-Lavigne, M. and Kidd, T. (1999). Slit proteins bind Robo receptors and have an evolutionarily conserved role in repulsive axon guidance. *Cell* **96**, 795-806.

Caton, A., Hacker, A., Naeem, A., Livet, J., Maina, F., Bladt, F., Klein, R., Birchmeier, C. and Guthrie, S. (2000). The branchial arches and HGF are growth-promoting and chemoattractant for cranial motor axons. *Development* **127**, 1751-1760.

Chandrasekhar, A. (2004). Turning heads: development of vertebrate branchiomotor neurons. *Dev. Dyn.* **229**, 143-161.

Chen, H., Chedotal, A., He, Z., Goodman, C. S. and Tessier-Lavigne, M. (1997). Neuropilin-2, a novel member of the neuropilin family, is a high affinity receptor for the semaphorins Sema E and Sema IV but not Sema III. *Neuron* **19**, 547-559.

Cordes, S. P. (2001). Molecular genetics of cranial nerve development in mouse. *Nat. Rev. Neurosci.* **2**, 611-623.

Corrales, J. D., Rocco, G. L., Blaess, S., Guo, Q. and Joyner, A. L. (2004). Spatial pattern of sonic hedgehog signaling through Gli genes during cerebellum development. *Development* **131**, 5581-5590.

Dalla Torre di Sanguinetto, S. A., Dasen, J. S. and Arber, S. (2008). Transcriptional mechanisms controlling motor neuron diversity and connectivity. *Curr. Opin. Neurobiol.* **18**, 36-43.
Devine, C. A. and Key, B. (2008). Robo-Slit interactions regulate longitudinal axon pathfinding in the embryonic vertebrate brain. *Dev. Biol.* **313**, 371-383.
Dillon, A. K., Fujita, S. C., Matise, M. P., Jarjour, A. A., Kennedy, T. E., Kollmus, H., Arnold, H.-H., Weiner, J. A., Sanes, J. R. and Kaprielian, Z. (2005). Molecular control of spinal accessory motor neuron/axon development in the mouse spinal cord. *J. Neurosci.* **25**, 10119-10130.
Dillon, A. K., Jevince, A. R., Hinck, L., Ackerman, S. L., Lu, X., Tessier-Lavigne, M. and Kaprielian, Z. (2007). UNC5C is required for spinal accessory motor neuron development. *Mol. Cell. Neurosci.* **35**, 482-489.
Dugan, J. P., Stratton, A., Riley, H. P., Farmer, W. T. and Mastick, G. S. (2011). Midbrain dopaminergic axons are guided longitudinally through the diencephalon by Slit/Robo signals. *Mol. Cell. Neurosci.* **46**, 347-356.
Englund, C., Steneberg, P., Falileeva, L., Xylourgidis, N. and Samakovlis, C. (2002). Attractive and repulsive functions of Slit are mediated by different receptors in the *Drosophila* trachea. *Development* **129**, 4941-4951.
Ericson, J., Thor, S., Edlund, T., Jessell, T. and Yamada, T. (1992). Early stages of motor neuron differentiation revealed by expression of homeobox gene *Islet-1*. *Science* **256**, 1555-1559.
Farmer, W. T., Altick, A. L., Nural, H. F., Dugan, J. P., Kidd, T., Charron, F. and Mastick, G. S. (2008). Pioneer longitudinal axons navigate using floor plate and Slit/Robo signals. *Development* **135**, 3643-3653.
Fraher, J. P., Dockery, P., O'Donoghue, O., Riedewald, B. and O'Leary, D. (2007). Initial motor axon outgrowth from the developing central nervous system. *J. Anat.* **211**, 600-611.
Garcia-Frigola, C., Carreres, M. I., Vegar, C., Mason, C. and Herrera, E. (2008). Zic2 promotes axonal divergence at the optic chiasm midline by EphB1-dependent and -independent mechanisms. *Development* **135**, 1833-1841.
Grieshammer, U., Le, M., Plump, A. S., Wang, F., Tessier-Lavigne, M. and Martin, G. R. (2004). SLIT2-mediated ROBO2 signaling restricts kidney induction to a single site. *Dev. Cell* **6**, 709-717.
Guthrie, S. (2007). Patterning and axon guidance of cranial motor neurons. *Nat. Rev. Neurosci.* **8**, 859-871.
Guthrie, S. and Lumsden, A. (1992). Motor neuron pathfinding following rhombomere reversals in the chick embryo hindbrain. *Development* **114**, 663-673.
Harvey, R. P. (1996). NK-2 homeobox genes and heart development. *Dev. Biol.* **178**, 203-216.
He, Z. and Tessier-Lavigne, M. (1997). Neuropilin is a receptor for the axonal chemorepellent semaphorin III. *Cell* **90**, 739-751.
Hiramoto, M., Hiromi, Y., Giniger, E. and Hotta, Y. (2000). The Drosophila Netrin receptor Frazzled guides axons by controlling Netrin distribution. *Nature* **406**, 886-889.
Hirsch, M.-R., Glover, J. C., Dufour, H. D., Brunet, J.-F. and Goridis, C. (2007). Forced expression of Phox2 homeodomain transcription factors induces a branchio-visceromotor axonal phenotype. *Dev. Biol.* **303**, 687-702.
Holland, S. J., Gale, N. W., Gish, G. D., Roth, R. A., Songyang, Z., Cantley, L. C., Henkemeyer, M., Yancopoulos, G. D. and Pawson, T. (1997). Juxtamembrane tyrosine residues couple the Eph family receptor EphB2/Nuk to specific SH2 domain proteins in neuronal cells. *EMBO J.* **16**, 3877-3888.
Holz, A., Kollmus, H., Ryge, J., Niederkofler, V., Dias, J., Ericson, J., Stoeckli, E. T., Kiehn, O. and Arnold, H. H. (2010). The transcription factors Nkx2.2 and Nkx2.9 play a novel role in floor plate development and commissural axon guidance. *Development* **137**, 4249-4260.
Hughes, T. R., Marton, M. J., Jones, A. R., Roberts, C. J., Stoughton, R., Armour, C. D., Bennett, H. A., Coffey, E., Dai, H., He, Y. D. et al. (2000). Functional discovery via a compendium of expression profiles. *Cell* **102**, 109-126.
Imondi, R. and Kaprielian, Z. (2001). Commissural axon pathfinding on the contralateral side of the floor plate: a role for B-class ephrins in specifying the dorsoventral position of longitudinally-projecting commissural axons. *Development* **128**, 4859-4871.
Imondi, R., Wideman, C. and Kaprielian, Z. (2000). Complementary expression of transmembrane ephrins and their receptors in the mouse spinal cord: a possible role in constraining the orientation of longitudinally projecting axons. *Development* **127**, 1397-1410.
Jacob, J., Hacker, A. and Guthrie, S. (2001). Mechanisms and molecules in motor neuron specification and axon pathfinding. *BioEssays* **23**, 582-595.
Jevince, A. R., Kadison, S. R., Pittman, A. J., Chien, C.-B. and Kaprielian, Z. (2006). Distribution of EphB receptors and ephrin-B1 in the developing vertebrate spinal cord. *J. Comp. Neurol.* **497**, 734-750.
Kadison, S. R., Murakami, F., Matise, M. P. and Kaprielian, Z. (2006). The role of floor plate contact in the elaboration of contralateral commissural projections within the embryonic mouse spinal cord. *Dev. Biol.* **296**, 499-513.
Kao, T. J. and Kania, A. (2011). Ephrin-mediated cis-attenuation of Eph Receptor signaling is essential for spinal motor axon guidance. *Neuron* **71**, 76-91.
Kidd, T., Bland, K. S. and Goodman, C. S. (1999). Slit is the midline repellent for the Robo receptor in *Drosophila*. *Cell* **96**, 785-794.
Kolodkin, A. L., Levengood, D. V., Rowe, E. G., Tai, Y.-T., Ginger, R. J. and Ginty, D. D. (1997). Neuropilin is a semaphorin III receptor. *Cell* **90**, 753-762.
Kramer, S., Kidd, T., Simpson, J. and Goodman, C. (2001). Switching repulsion to attraction: changing responses to slit during transition in mesoderm migration. *Science* **292**, 737-740.
Labrador, J. P., O'Keefe, D., Yoshikawa, S., McKinnon, R. D., Thomas, J. B. and Bashaw, G. J. (2005). The homeobox transcription factor even-skipped regulates netrin-receptor expression to control dorsal motor-axon projections in *Drosophila*. *Curr. Biol.* **15**, 1413-1419.
Landgraf, M., Roy, S., Prokop, A., VijayRaghavan, K. and Bate, M. (1999). *even-skipped* determines the dorsal growth of motor axon in *Drosophila*. *Neuron* **22**, 43-52.
Layden, M. J., Odden, J. P., Schmid, A., Garces, A., Thor, S. and Doe, C. Q. (2006). Zfh1, a somatic motor neuron transcription factor, regulates axon exit from the CNS. *Dev. Biol.* **291**, 253-263.
Lee, R., Petros, T. J. and Mason, C. A. (2008). Zic2 regulates retinal ganglion cell axon avoidance of ephrinB2 through inducing expression of the guidance receptor EphB1. *J. Neurosci.* **28**, 5910-5919.
Lieberam, I., Agalliu, D., Nagasawa, T., Ericson, J. and Jessell, T. M. (2005). A Cxcl12-Cxcr4 chemokine signaling pathway defines the initial trajectory of mammalian motor axons. *Neuron* **47**, 667-679.
Long, H., Sabatier, C., Ma, L., Plump, A., Yuan, W., Ornitz, D. M., Tamada, A., Murakami, F., Goodman, C. S. and Tessier-Lavigne, M. (2004). Conserved roles for Slit and Robo proteins in midline commissural axon guidance. *Neuron* **42**, 213-223.
Lopez-Bendito, G., Flames, N., Ma, L., Fouquet, C., Meglio, T. D., Chedotal, A., Tessier-Lavigne, M. and Marin, O. (2007). Robo1 and Robo2 cooperate to control the guidance of major axonal tracts in the mammalian forebrain. *J. Neurosci.* **27**, 3395-3407.
Lu, W., van Eerde, A. M., Fan, X., Quintero-Rivera, F., Kulkarni, S., Ferguson, H., Kim, H. G., Fan, Y., Xi, Q., Li, Q. G. et al. (2007). Disruption of ROBO2 is associated with urinary tract anomalies and confers risk of vesicoureteral reflux. *Am. J. Hum. Genet.* **80**, 616-632.
Maness, P. F. and Schachner, M. (2007). Neural recognition molecules of the immunoglobulin superfamily: signaling transducers of axon guidance and neuronal migration. *Nat. Neurosci.* **10**, 19-26.
Maro, G. S., Vermeren, M., Voiculescu, O., Melton, L., Cohen, J., Charnay, P. and Topilko, P. (2004). Neural crest boundary cap cells constitute a source of neuronal and glial cells of the PNS. *Nat. Neurosci.* **7**, 930-938.
Mastick, G. S., Farmer, W. T., Altick, A. L., Nural, H. F., Dugan, J. P., Kidd, T. and Charron, F. (2010). Longitudinal axons are guided by Slit/Robo signals from the floor plate. *Cell Adh. Migr.* **4**, 337-341.
Mauti, O., Domanitskaya, E., Andermatt, I., Sadhu, R. and Stoeckli, E. T. (2007). Semaphorin6A acts as a gate keeper between the central and the peripheral nervous system. *Neural Dev.* **2**, 28.
McFarlane, S. (2003). Metalloproteases: carving out a role in axon guidance. *Neuron* **37**, 559-562.
Moret, F., Renaudot, C., Bozon, M. and Castellani, V. (2007). Semaphorin and neuropilin co-expression in motoneurons sets axon sensitivity to environmental semaphorin sources during motor axon pathfinding. *Development* **134**, 4491-4501.
Pabst, O., Herbrand, H. and Arnold, H. H. (1998). Nkx2-9 is a novel homeobox transcription factor which demarcates ventral domains in the developing mouse CNS. *Mech. Dev.* **73**, 85-93.
Pabst, O., Rummelies, J., Winter, B. and Arnold, H.-H. (2003). Targeted disruption of the homeobox gene *Nkx2. 9* reveals a role in development of the spinal accessory nerve. *Development* **130**, 1193-1202.
Palmer, A. and Klein, R. (2003). Multiple roles of ephrins in morphogenesis, neuronal networking, and brain function. *Genes Dev.* **17**, 1429-1450.
Pattyn, A., Hirsch, M.-R., Goridis, C. and Brunet, J.-F. (2000). Control of hindbrain motor neuron differentiation by the homeobox gene Phox2b. *Development* **127**, 1349-1358.
Pfaff, S. L., Mendelsohn, M., Stewart, C. L., Edlund, T. and Jessell, T. M. (1996). Requirement for LIM homeobox gene *Isl1* in motor neuron generation reveals a motor neuron-dependent step in interneuron differentiation. *Cell* **84**, 309-320.
Plump, A., Erskine, L., Sabatier, C., Brose, K., Epstein, C., Goodman, C., Mason, C. and Tessier-Lavigne, M. (2002). Slit1 and Slit2 cooperate to prevent premature midline crossing of retinal axons in the mouse visual system. *Neuron* **33**, 219-232.
Reeber, S. L., Sakai, N., Nakada, Y., Dumas, J., Dobrenis, K., Johnson, J. E. and Kaprielian, Z. (2008). Manipulating Robo expression in vivo perturbs commissural axon pathfinding in the chick spinal cord. *J. Neurosci.* **28**, 8698-8708.
Ricano-Cornejo, I., Altick, A. L., Garcia-Pena, C. M., Nural, H. F., Echevarria, D., Miquelajauregui, A., Mastick, G. S. and Varela-Echavarria, A. (2011). Slit-Robo signals regulate pioneer axon pathfinding of the tract of the postoptic commissure in the mammalian forebrain. *J. Neurosci. Res.* **89**, 1531-1541.
Ruiz de Almodovar, C., Lambrechts, D., Mazzone, M. and Carmeliet, P. (2009). Role and therapeutic potential of VEGF in the nervous system. *Physiol. Rev.* **89**, 607-648.

Schachter, P. P., Ayesh, S., Schneider, T., Laster, M., Czerniak, A. and Hochberg, A. (2002). Expression of kinase genes in primary hyperparathyroidism: adenoma versus hyperplastic parathyroid tissue. *Surgery* **132**, 1094-1099.
Schneider, V. A. and Granato, M. (2003). Motor axon migration: a long way to go. *Dev. Biol.* **263**, 1-11.
Schneider, V. A. and Granato, M. (2006). The myotomal diwanka (lh3) glycosyltransferase and type XVIII collagen are critical for motor growth cone migration. *Neuron* **50**, 683-695.
Schubert, W. and Kaprielian, Z. (2001). Identification and characterization of a cell surface marker for embryonic rat spinal accessory motor neurons. *J. Comp. Neurol.* **439**, 368-383.
Sharma, K. and Peng, C.-Y. (2001). Spinal motor circuits: Merging development and function. *Neuron* **29**, 321-324.
Sharma, K., Sheng, H. Z., Lettieri, K., Li, H., Karavanov, A., Potter, S., Westphal, H. and Pfaff, S. L. (1998). LIM homeodomain factors Lhx3 and Lhx4 assign subtype identities for motor neurons. *Cell* **95**, 817-828.
Shiau, C. E. and Bronner-Fraser, M. (2009). N-cadherin acts in concert with Slit1-Robo2 signaling in regulating aggregation of placode-derived cranial sensory neurons. *Development* **136**, 4155-4164.
Shirasaki, R. and Pfaff, S. L. (2002). Transcriptional codes and the control of neuronal identity. *Ann. Rev. Neurosci.* **25**, 251-281.
Snider, W. D. and Palavali, V. (1990). Early axon and dendritic outgrowth of spinal accessory motor neurons studied with DiI in fixed tissues. *J. Comp. Neurol.* **297**, 227-238.
Stanfel, M. N., Moses, K. A., Schwartz, R. J. and Zimmer, W. E. (2005). Regulation of organ development by the NKX-homeodomain factors: an NKX code. *Cell. Mol. Biol. (Noisy-le-grand)* **51 Suppl.**, OL785-OL799.
Swartz, M. E., Eberhart, J., Pasquale, E. B. and Krull, C. E. (2001). EphA4/ephrin-A5 interactions in muscle precursor cell migration in the avian forelimb. *Development* **128**, 4669-4680.
Tian, J., Mahmood, R., Hnasko, R. and Locker, J. (2006). Loss of Nkx2.8 deregulates progenitor cells in the large airways and leads to dysplasia. *Cancer Res.* **66**, 10399-10407.
Vermeren, M., Maro, G. S., Bron, R., McGonnell, I. M., Charnay, P., Topilko, P. and Cohen, J. (2003). Integrity of developing spinal motor columns is regulated by neural crest derivatives at motor exit points. *Neuron* **37**, 403-415.
Vosshall, L. B., Wong, A. M. and Axel, R. (2000). An olfactory sensory map in the fly brain. *Cell* **102**, 147-159.
Wang, H., Zhu, Y. Z., Wong, P. T., Farook, J. M., Teo, A. L., Lee, L. K. and Moochhala, S. (2003). cDNA microarray analysis of gene expression in anxious PVG and SD rats after cat-freezing test. *Exp. Brain Res.* **149**, 413-421.
Wilson, S. I., Shafer, B., Lee, K. J. and Dodd, J. (2008). A molecular program for contralateral trajectory: Rig-1 control by LIM homeodomain transcription factors. *Neuron* **59**, 413-424.
Ye, B. Q., Geng, Z. H., Ma, L. and Geng, J. G. (2010). Slit2 regulates attractive eosinophil and repulsive neutrophil chemotaxis through differential srGAP1 expression during lung inflammation. *J. Immunol.* **185**, 6294-6305.
Ypsilanti, A. R., Zagar, Y. and Chedotal, A. (2010). Moving away from the midline: new developments for Slit and Robo. *Development* **137**, 1939-1952.
Yuan, L., Hillman, J. D. and Progulske-Fox, A. (2005). Microarray analysis of quorum-sensing-regulated genes in Porphyromonas gingivalis. *Infect. Immun.* **73**, 4146-4154.
Yuan, W., Zhou, L., Chen, J.-h., Wu, J., Rao, Y. and Ornitz, D. (1999). The mouse Slit family: secreted ligands for Robo expressed in patterns that suggest a role in morphogenesis and axon guidance. *Dev. Biol.* **212**, 290-306.

Table S1. Genes that are differentially expressed in *Nkx2.9*-deficient mouse embryos			
Fold change	**Regulation**	**Gene description**	**GenBank**
10.5	Up	inactive X specific transcripts	BC051222
4.6	Down	eukaryotic translation initiation factor 2, subunit 3, structural gene Y-linked	BC043656
4.3	Down	jumonji, AT rich interactive domain 1D (Rbp2 like)	AF127244
3.7	Down	DEAD (Asp-Glu-Ala-Asp) box polypeptide 3, Y-linked	BC021453
3.6	Down	ubiquitously transcribed tetratricopeptide repeat gene, Y chromosome	AF057367
2.9	Down	homeo box C8	X07646
2.9	Down	RIKEN cDNA 4922502B01 gene	AK013705
2.4	Down	homeo box C6	X16511
2.4	Down	calbindin-28K	M21531
2.3	Down	homeo box D8	NM_008276.2
2.2	Down	neuromedin S	AB164466
2.1	Up	forkhead box D1	L38607
2.0	Down	otoraplin	AJ243939
2.0	Down	diacylglycerol kinase kappa	BC075627
2.0	Down	homeo box B9	BC100743
1.9	Down	carbonic anhydrase 10	AB080741
1.9	Down	V-set and transmembrane domain containing 2A	BC027127
1.9	Up	Tex17	AF285579
1.9	Down	Riken cDNA C130021I20 gene	AK147796
1.9	Down	homeo box A6	BC119105
1.9	Down	protein tyrosine phosphatase, non-receptor type 3	NM_011207.2
1.9	Down	MACRO domain containing 2	NC_000068.6
1.8	Up	SLIT and NTRK-like family, member 6	BC145927
1.8	Up	solute carrier family 38, member 4	AY027919
1.8	Down	dehydrogenase/reductase (SDR family) member 3	BC010972
1.8	Down	neurotrophin 3	BC065785
1.8	Down	latexin	D88769
1.8	Down	RIKEN cDNA 6430550H21 gene	BC062956
1.8	Up	decorin	BC132521
1.8	Down	LIM domain binding 2	U89489
1.8	Down	MAM domain containing glycosylphosphatidylinositol anchor 2	AY371925
1.8	Down	protein tyrosine phosphatase, non-receptor type 3	NM_011207.2
1.8	Down	cadherin 7, type 2	BC083189
1.8	Up	wingless-related MMTV integration site 5A	BC018425
1.7	Down	hemicentin 1	NM_001024720.3

1.7	Down	CUB and Sushi multiple domains 3	NM_001081391.2
1.7	Down	visinin-like 1	AY101375
1.7	Down	leucine rich repeat containing 4C	BC094588
1.7	Down	cadherin 9	NM_009869.1
1.7	Down	MACRO domain containing 2	NC_000068.6
1.7	**Down**	**Adamts3**	**NM_177872.2**
1.7	Down	SLIT and NTRK-like family, member 2	BC111888
1.7	Down	protein phosphatase 1, regulatory (inhibitor) subunit 1C	BC120706
1.7	Down	metallophosphoesterase domain containing 2	BC020182
1.7	Down	aldehyde dehydrogenase family 1, subfamily A2	BC075704
1.7	Down	CUB and Sushi multiple domains 3	NM_001081391.2
1.7	Up	metallothionein 2	BC031758
1.7	Down	tachykinin 1	D17584
1.7	**Down**	**roundabout homolog 2 (Drosophila)**	**DQ533876**
1.7	Up	gene model 784, (NCBI)	DQ192038|BC076625
1.6	Down	KH domain containing, RNA binding, signal transduction associated 2	BC132117
1.6	Up	meiotic nuclear divisions 1 homolog (S. cerevisiae)	BC027741
1.6	Down	zinc finger protein 804A	BC035535
1.6	Up	RIKEN cDNA 2610301F02 gene	AK011952.1
1.6	Up	vitronectin	BC012690
1.6	Up	RIKEN cDNA 3100002J23 gene	BC117741|BC126964|BC094630
1.6	Down	SLIT and NTRK-like family, member 2	AK141924
1.6	Down	neuritin 1	BC035531
1.6	Down	PNMA-like 2	NM_001099636.2
1.6	Up	small nucleolar RNA, C/D box 16A	AF357363
1.6	Down	solute carrier family 17 (Na-dependent inorganic phosphate cotransporter), member 6	BC038375
1.6	Up	versican	D16263
1.6	Up	chemokine (C-X-C motif) ligand 12	D43804
1.6	Down	synaptic vesicle glycoprotein 2c	BC132111|U24700|AK173092
1.6	Down	glutamate receptor, ionotropic, AMPA1 (alpha 1)	BC056397
1.6	Up	sulfatase 1	AY101178
1.6	Up	myeloblastosis oncogene-like 1	L35261
1.6	Up	RIKEN cDNA 1810011O10 gene	BC016562
1.6	Down	potassium voltage-gated channel, Shal-related family, member 2	AB045326
1.6	Down	transmembrane protein 108	BC052085
1.6	Down	ubiquitin specific peptidase 29	AF229257
1.6	Up	dopa decarboxylase	AF071068

Genes exhibiting a fold change greater than 1.5 in *Nkx2.9* null mice as compared with WT littermates.